Research Article
doi: 10.1590/01047760202329013208
vol(29), 2023

CERNE

Appraisal of arp images and machine learning to detect *Sapajus nigritus* attacks on loblolly's pine stands in Southern Brazil

Carla Talita Pertille[1]✤, Marcos Benedito Schimalski[2], Veraldo Liesenberg[3], Vilmar Picinatto Filho[4], Mireli Moura Pitz[5], Fabiani das Dores Abati Miranda[6]

[1]Federal University of Paraná, Curitiba, Brazil
[2]Federal University of Santa Catarina, Florianópolis, Brazil
[3]State University of Santa Catarina, Florianópolis, Brazil
[4]Sumatra Inteligência Ambiental Santa Catarina, Lages, Brazil
[5]Klabin S.A. Lages, Brazil
[6]Federal University of Technology – Paraná, Curitiba, Brazil

FOREST MANAGEMENT

ABSTRACT

Background: This study aimed to evaluate UAV images of *Pinus taeda* L. stands for classifying trees attacked by *Sapajus nigritus* in Southern Brazil. UAV images were acquired on March 2018, using a DJI Phantom Pro 4 over 18.73 hectares. We evaluated different band compositions and vegetation indices. Using photo interpretation based on the color of the crown and field measurements, the trees were manually labeled as not attacked, dead, and attacked. The classified trees were divided into training (75%) and validation (25%), considering three tree crown diameters (0.5, 1, and 1.5 m) and three region-oriented classification algorithms. The classification accuracy was assessed by overall accuracy and the kappa index.

Results: A total of 3,773 trees were manually detected, of which 39% were attacked, 5% died and 56% were not attacked. The results also indicated that the best-chosen diameter was 0.5 meters, the best classifier algorithm was the SVM, and the highest accuracy was represented by the composition of the ExG index associated with the original spectral bands.

Conclusion: We argue that the attacks can be monitored using UAV images and such results provide insights for forest management initiatives.

Key words: UAV; photogrammetry; forest health.

HIGHLIGHTS

The ExG was the best index for analyzing the forest health of *Pinus taeda* L.

PERTILLE, C.T.; SCHIMALSKI, M.B.; LIESENBERG, V.; FILHO, V.P.; PITZ, M.M.; MIRANDA, F.D.A. USE OF *ACACIA AURICULIFORMIS* Appraisal of arp images and machine learning to detect *Sapajus nigritus* attacks on Loblolly's pine stands in southern Brazil. CERNE, v.29, e-103208, doi: 10.1590/01047760202329013208

✤Corresponding author: carla.pertille@ufpr.br Received: December, 22/2022 Accepted: April, 23/2023

Open Access
CERNE
ISSN 0104-7760
UFLA UNIVERSIDADE FEDERAL DE LAVRAS

INTRODUCTION

Sapajus nigritus Kerr (1972), popularly known as capuchin monkey, is a species of primate found in South and South-east Brazil Atlantic forest domain. Due to its omnivorous diet, during periods of food scarcity due to low fruiting season in the Atlantic Forest (Liebsch et al., 2008; Tujague and Janson, 2017), *Sapajus nigritus* supplemented its diet with other resources evenly distributed in the habitat and presented in forest remnants (Di Bitetti, 2019). However, more recently, *Sapajus nigritus* identified a new food source in the exudation of *Pinus* spp. trees (Rocha, 2000; Retslaff et al, 2020). To gain access to exudation, *Sapajus nigritus* removes the bark causing two types of damage: windowing (partial stripping of the bark from the trunk) and girdling (stripping of the bark in a ring around the trunk). Regardless of the type of damage, phloem conduction is partially interrupted, causing the upper canopy to dry out. Consequently, it may favours the occurrence of pathogens and, after some time, the combination of these factors can even cause the death of the tree (Koehler and Firkoski, 1996; Mikich and Liebsh, 2009; Mikich and Liebsch, 2014; Liebsch et al., 2015; Rocha, 2000; Retslaff *et al.*, 2020). Considering the importance of the genus *Pinus* spp. in the Brazilian forest sector, whose plantations represent 17% of planted forests (Ibá, 2021), remote sensing initiatives for forest protection of such stands are extremely important.

The use of remote sensing and aerial images obtained by Unmanned Aerial Vehicles (UAV) has been standing out and evolving into precision farming applications, including tree health detection (Ishida et al., 2018). Forest health is one of the criteria used to protect forest stands, given the records of pest attacks and the occurrence of diseases in plantations in Brazil since the 1990s. However, studies using using remote sensing resources and data, such as aerial images obtained by UAVs, to identify and quantify the impact of the Sapajus nigritus on forest plantations are still scarce. Following this theme, recent studies such as Dash et al. (2018) provided a substantial review showing the physiological stress in forest trees caused by biotic and abiotic factors. Sylvain et al. (2019) showed how useful advanced machine learning methods, such as deep Convolutional Neural Networks (CNNs), have achieved unprecedented performance in object recognition and classification tasks. In their study, such approach was useful to detect the health status and functional type of trees. Interestingly, Safonova et al. (2020) demonstrated the significance of remote sensing data in controlling the invasion of *Polygraphus proximus* Blandford on catastrophic damage to fir forests (*Abies sibirica* Ledeb) in Russia, especially in Central Siberia. Similarly, Moriya et al. (2021), showed the importance of UAV measures for mapping diseases in citrus and how useful such information can be used for land monitoring and cultural practices at stand and farm level.

This research was based on the application of remote sensing technologies to detect the attack of *Sapajus nigritus* on forest plantations, aiming to classify individual trees of *Pinus taeda* L. as attacked, non-attacked and dead trees, using UAV images and machine learning algorithms. Our study area is a typical loblolly pine stand located in Southern Brazil.

MATERIAL AND METHODS

Description of the area

The research was conducted in the municipality of Bocaina do Sul, in the state of Santa Catarina (Southern Brazil), with central coordinates 27°41'32.41" S and 49°57'46.06" W (Figure 1). According to Alvares et al. (2013), the climate of the location is Cfb type (humid subtropical mesothermal climate), by the Köppen classification. The average temperature is 16.5 °C, the average relative humidity of 79.3%, and precipitation is well distributed throughout the year, with an annual average of 1,500 mm.

The forest stands evaluated as indicated by a Brazilian forestry company, with 236.21 hectares of *Pinus taeda* L. plantations with ages ranging from 12–18 years for pulp and paper production. The spacing used was 3 meters × 2.5 meters, without silvicultural intervention, that is, without pruning and thinning.

Flight execution

The flight planning was elaborated for two nearby areas with attack records, totaling 18.73 hectares, of which 9.23 hectares were for Area 1 and 9.50 hectares for Area 2, with 12 and 13 years old, respectively (Figure 1). Both areas are very similar each other in terms of structural characteristics and were reported with a higher incidence of attack by the company. Both areas were surveyed individually for optimizing the data acquisition. For aerial coverage, aerial imaging was carried out in March 2018, using a quadcopter-type UAV, model DJI Phantom 4 Pro, equipped with a multispectral sensor type CMOS (Complementary Metal-Oxide Semiconductor) of 1" with 20 megapixels of spatial resolution (5 micrometers pixel) and focal length of 8.8 mm. The images were captured in the visible range: blue (0.40-0.58 nm), green (0.50-0.65 nm), and red (0.59-0.68 nm). A Global Navigation Satellite System (GNSS), i.e., Leica Viva GS15 was used to collect ground control points (GCPs), favoring the collection of georeferenced images. We adopted a flight hight of 120m because the study area showed a gentle topography and is allowed by current Brazilian legislation.

The flights were carried out in the early afternoon period, between 2 p.m. and 3 p.m., to minimize the shadow effect. Flight speed was determined according to weather conditions (exposure to luminosity and adverse weather conditions) being 7 $m.s^{-1}$, following a linear route according to Redweik (2007) orientation. The lateral and frontal overlaps were 80% and 85% in agreement with Mancini et al. (2013). After image collection, photogrammetric processing was performed at the Agisof Metashape Professional (Agisoft LLC, St. Petersburg, Russia), in which the corrections related to automatic aerial triangulation, generation of the dense point cloud, the rectification of images, and acquisition of the mosaic were carried out.

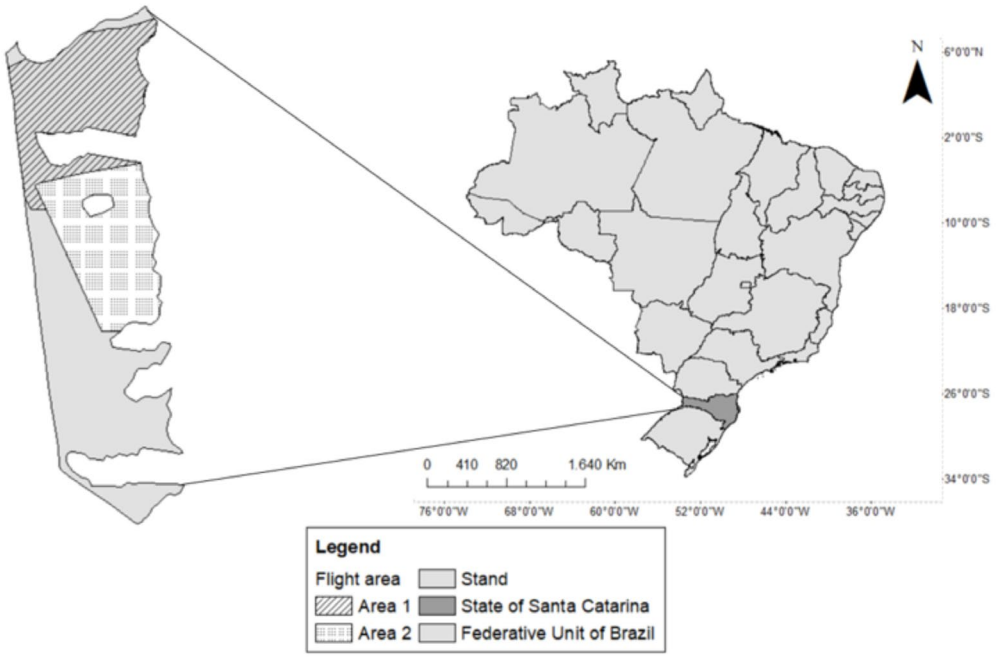

Figure 1: Location of the Santa Catarina State within Brazil with Boundary of the forest stand and the indication of the surveyed area by UAV. *Note: Local coordinates have been omitted for confidentiality reasons.

Processing data

Vegetation indices were chosen according to the spectral bands (only in the visible range) and for presenting satisfactory results in the separation of soil and vegetation, according to the consulted literature (Table 1).

To highlight the spectral behavior of the attacked trees, different band compositions were selected for the twothree areas using the red and blue bands of the orthomosaics and the vegetation indexes, which replaced the green band for identifying attacked, not attacked, and dead trees as function of the color of the crown. Thus, the compositions were as follows: Composite 1: band Red, BGI Index, and band Blue;; Composite 2: band Red, ExG index, and band Blue; Composite 3: band Red, GLI Index, and band Blue; Composite 4: band Red, RGI index, and band Blue and 5: band Red, TGI Index, and band Blue. In addition to the compositions, orthomosaics were also used (Figure 2).

To identify the trees, photointerpretation parameters, such as color tone, brightness, and texture, were used, for establishing three qualitative classes of damage per tree, which were: green crown (tree without damage); yellowish/reddish crown (a tree with recent or former attack); gray crown (dead tree). The above parameters were set based on field surveys. A total of ten circular plots were distributed randomly in the two areas, five each. The size varies according to the presence or not of the attack and ranged from 5 to 10m. All trees were surveyed, and each crown was assigned with a point that was then labeled qualitatively into attacked, not attacked, and dead trees, in addition to the description of the type of damage (girdling and/or windowing) and the number of visible damages per tree. In each sample plot, the central coordinate was obtained through GNSS signal receivers assurin a perfect match with the images. After, we perform a segmentation using the mean shift algorithm available in a GIS environment (ESRI, 2021). The segments were then submitted to a supervised classification approach oriented to segments aiming to obtain the crown coverage and the soi contribution.

Data analysis

A total of 3,773 were labeled into attacked (1,478), non-attacked (2,098) and dead (197). The dataset was randomly divided into 75% training and 25% validation (Jensen, 2007; Pereira and Centeno, 2017). For the 3,773 points, three circle sizes with 0.5 m, 1 m, and 1.5 m radius were generated. These values were considered to obtain different levels of crown coverage and to verify whether this variation in the circle sizes could contribute to the possibility of separating the trees according to their phytosanitary condition. The algorithms Maximum Likelihood (Maxver), Support Vector Machine (SVM), and Random Tree (RT) were applied and evaluated.

The assertiveness of the supervised classification by the three algorithms was verified by the error matrix and by the values of the overall accuracy and kappa index. Overall accuracy refers to the total number of correctly classified samples (that is, the sum of true positives for all classes) divided by the total number of samples. The Kappa index evaluates the agreement of the prediction with the true class. This metric compares an observed accuracy with an expected accuracy (that is, it considers the random chance of sorting correctly) (Nevalainen et al., 2017).

Table 1: Vegetation indices derived for a stand of Pinus taeda L. attacked by Sapajus nigritus located in Bocaina do Sul – Santa Catarina.

Vegetation Index (VI)	Equation	Reference
BGI	B3/B2	Zarco-Tejada et al. (2005)
ExG	2 *B2 – B1 – B3	Woebbecke et al. (1995)
GLI	(2* B3 – B1 – B2) – (2* B3+ B1+ B2)	Louhaichi et al. (2001)
RGI	B1/B2	Coops et al. (2006)
TGI	- 0,5 * [(B1 – B3) * (B1 –B2) – (B1 – B3) * (B1 – B2)]	Hunt et al. (2011)

Where, BGI : Blue-Green Pigment Index; ExG: Excess green, GLI: Green Leaf Index; RGI: Red-green index, TGI: Triangular Greenness Index, B1: red (0.59-0.68 nm), B2: green (0.50-0.65 nm), and B3: blue (0.400.58 nm).

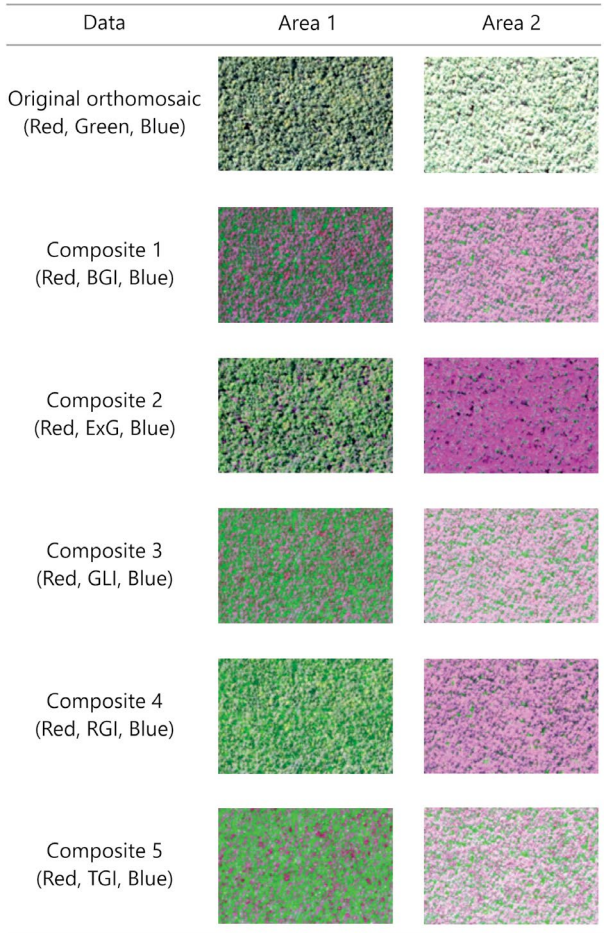

Figure 2: Subsets used for the evaluated areas for a stand of *Pinus taeda* L. attacked by *Sapajus nigritus* located in Bocaína do Sul – Santa Catarina.

RESULTS

The use of vegetation indices (VI) made it possible to visually differentiate the health status of the trees (attacked, not attacked and dead) in the areas analyzed in manual detection. The scale of values of each vegetation index varied, and the ExG presented the highest values for all classes with the TGI presenting the lowest values. Thus, for the two evaluated areas, the ExG index showed higher separability between vegetation and bare soil. It also provided greater separation between the attacked, non-attacked, and dead trees. When comparing the attacked and non-attacked trees, the reflectance decreased, lowering the VI values (Figure 3). For dead and non-attacked trees, high reflectance values were found, causing therefore a misclassification in these two classes. On the other hand, the area classified as bare soil presented low values in all VI in the evaluated areas due to largely closed canopies needlelike leaves.

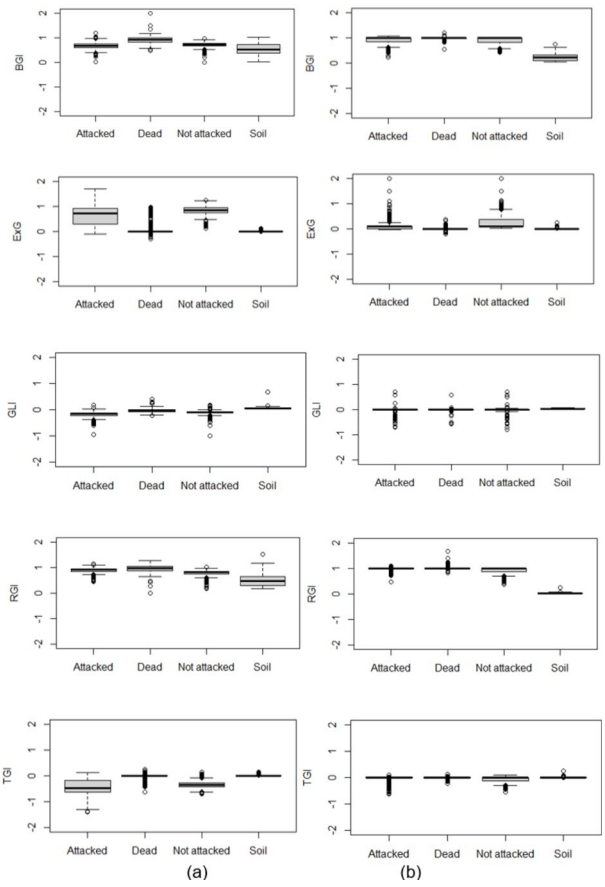

Figure 3: Boxplot of vegetation indices (VI) calculated with training classes for the two areas (a) Area 1 and (b) Area 2, respectively.

The manual classification of the trees (Figure 4) revealed differences for each analyzed area and the highest percentage of trees attacked was identified in Area 1 (41.5%).

Area 2 presented the largest number of non-attacked trees (59.3%). However, when the attack is recent, the crown still presents non-attacked behavior with apparent green needlelike leaves upon the sensor perspective.

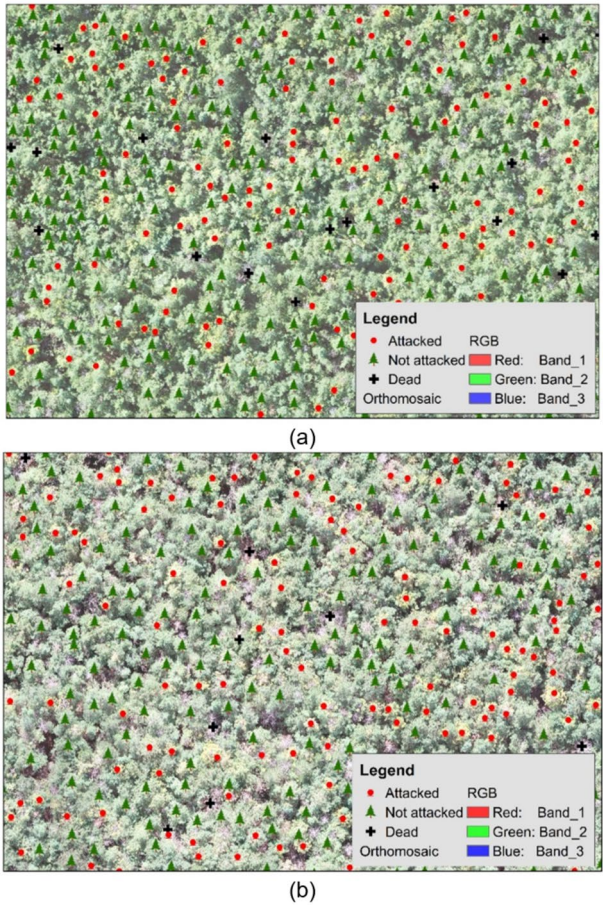

Figure 4: Manual detection of trees as a function of their sanity for area 1 (a) and area 2 (b) analyzed from a *Pinus taeda* L. stand located in Bocaina do Sul – SC.

The classification obtained with the 0.5 m samples showed superior statistics (i.e., overall accuracy and kappa index) at 80%, and composition 2 showed the highest values, with 88% overall accuracy and an 83% kappa index. For the 1 m samples, the RT and SVM methods were superior (with overall accuracy ranging from 0.66 to 0.79, and kappa index between 0.46 and 0.64, respectively). Maxver presented an overall accuracy ranging from 0.57 to 0.61 and kappa index below 54%. For the 1.5 m samples, compositions 1, 2, and 3 showed evaluation statistics above 80% whereas the other images had results below 70%. In Area 2, the classification obtained with circle samples with a 0.5 m radius showed statistics between 67 and 91%. The classification in true colors had greater accuracy than the classification tested with the vegetation indexes, considering the SVM method. For samples with a 1 m radius, the Maxver method was noticeably inferior and the performance of the RT method, which was significant in compositions 1, 3, 4, and 5, stood out, with overall accuracy and kappa index greater than 60%. The SVM method provided the best classification for the orthomosaic in true colors and with the composition with ExG. Samples with a larger radius (1.5 m) had statistics below 75%.

The classification using SVM method for the first area revealed that the best distinction of the attacked trees occurred in the classification with the ExG index composition (Figure 4). In all combinations, the samples of the non-attacked trees were misclassied with bare soil. The best representativeness of attacked trees occurred with the lowest errors of omission and commission among classes, and the higher accuracy values (I.e., overall accuracy of 0.88 and kappa of 0.83) was achieved choosing the ExG as an input for the first area (Figure 5). Interestingly, area 2 showed better performance usingthe use of true colors for differentiating attacked from non-attacked trees showing the smallest errors of omission or commission. With the use of BGI, dead trees were identified as attacked and with ExG, they were misclassified as non-attacked trees.

DISCUSSION

According to the analyses performed in the two areas, in the initial phase, no visual signs of attack are identified since this damage occurs in the trunk of the tree while the crown remains green upon the UAV perspective. However, over time, the symptoms of the attack evolve, and the needlelike leaves become yellowish and/or reddish (Vogelmann et al., 2009). According to the authors, if the attack progresses to severe stages, it could even cause the death of attacked tree. Regarding the compositions tested with the different VI (Figure 2), the difference in the number attacked and non-attacked trees for the two selected areas analyzed contributed to evidence the different behaviors and the difficulty of classifying attacked from non-attacked trees once the injury was caused recently. According to the results reported by Liebsch et al. (2015), windowing is the least harmful damage in terms of wood increment, however, with greater damage to the quality of the wood. The girdling is mostly responsible for the partial drying of the individuals, disrupting the exudation transport above the lesion.

The VI derived for each study area and their respective relationship with the training classes is restricted to the visible spectrum. The analysis of the VI for the evaluated classes showed differences according to the analyzed spectral range (Figure 3). Such variation is due to leaf biochemical properties, especially those related with the chlorophyll content that is mostly affected by possible stress caused by the attack. Such behavior and variability also occurred in the evaluation of the impact of *Ips topographus* Linnaeus attack when analyzing the spectral reflectance characteristics of *Picea abies* L. developed by Abdullah et al. (2018). The inclusion of additional cameras operating in the near-infrared or even shortwave infrared bands would surely contribute for a better assessment of the health of the attacked trees and are suggested for future studies. However, some challenges may still occur since the typical green color may remain some days after the injury, bringing some additional challenges and encouraging further studies.

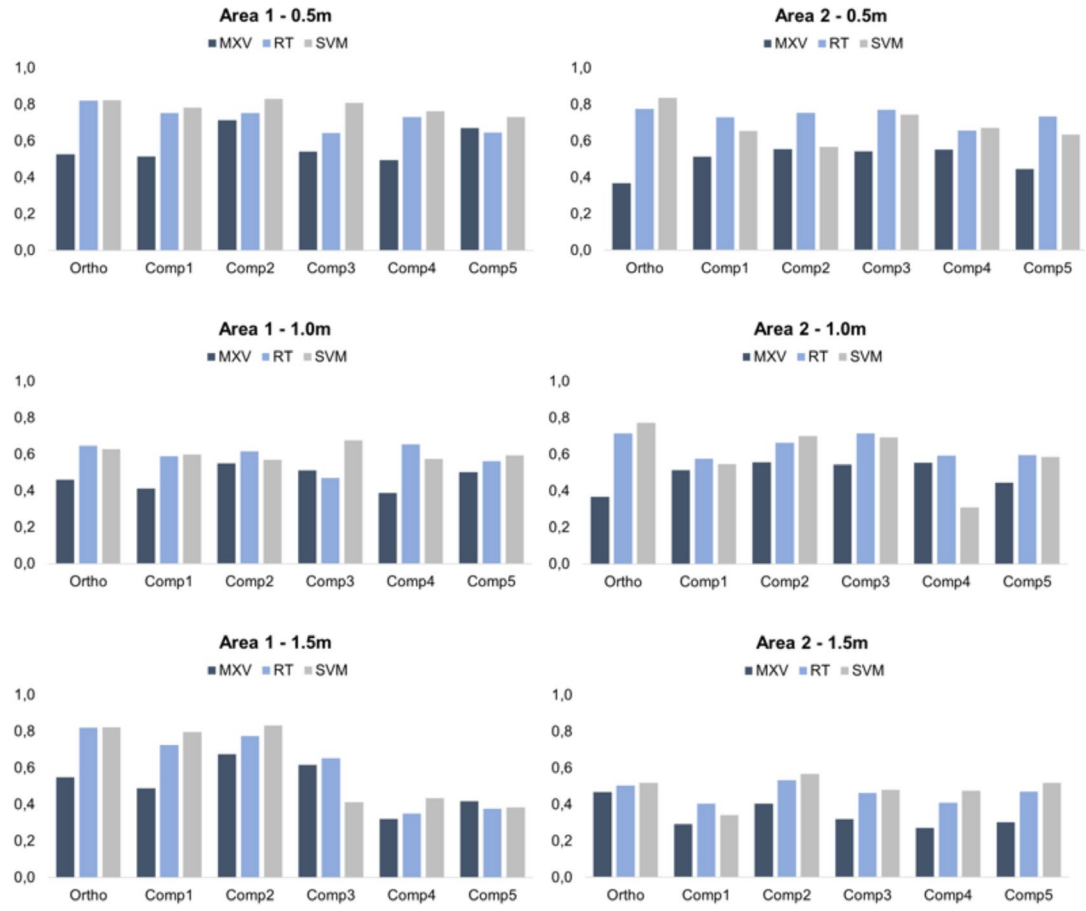

Figure 5: Kappa index of the tested algorithms for the classification of the forest health of *Pinus taeda* L. Where: MXV: Maxver; RT: Random Tree; SVM: Support Vector Machine; Ortho: orthophoto; Comp1: R-BGI-B; Comp2: R-ExG-B; Comp3: R-GLI-B; Comp4: R-RGI-B e Comp5: R-TGI-B. The details of the compositions are further detailed in Figure 2.

The manual classification of trees into attacked, non- attacked provided relevant information for the analyzed area in form of mapsthat can be used by foresters (Figure 4). Such information can provide potential analysis and allow the identification of trees that will have limitation in the growth rate. As a consequence, a decision about eventually removing attacked trees as suggested by Hansen et al. (2010) can be taken. Thus, note the importance of monitoring the attacked trees, especially in the initial stage of the development of the tree that could be then labeled for pruning and thinning, supporting management initiatives and, enabling the adoption of strategies to reduce the impact of the attack of this primate.

From the selected classification algorithms , we noticed that the best accuracy were obtained with a radius circle of 0.5 m and using SVM for area 1. Such achievents are in agreement with those reported by Behmann et al. (2014) when studying the detection of the influence of water stress on barley plants using VI and SVM. In this research, to the plants were distinguished between healthy and stressed plants. In general, the reported results indicate that for all tested spectral compositions, the data of the samples generated with circles with a radius of 0.5 m provided the best performance. In addition, classifying images using SVM method produced the highest overall precisions, with overall accuracy ranging from 0.56 to 0.83 and 0.73 to 0.91 for the kappa index in both areas as shown in Figure 5.

The variation in the combinations and areas tested is due to the spectral bands evaluated in each VI since the BGI does not use red in its calculation and the ExG covers the three bands of the visible spectrum, presenting greater sensitivity to the differences of reflectance between tree individuals with signs of attack and without damage. In the other compositions, the attacked trees were erroneously classified as non-attacked, especially in crowns with a transition from greenish tones (characterizing individuals without damage) to yellowish tones (signaling initial symptoms of attack). The bare soil was misclassified with the other classes by crown conditions and by the presence of dry vegetation.

The performance of the tested algorithms is related to some specific characteristics, as explained below. One factor that can influence this process refers to isolating individual trees and distinguishing brightness between the canopies and the bare soil. This depends on the spatial resolution of the image used and the size of the canopies. Images with ultra-high spatial resolution, that is, with GSD between 5 to 15 cm, show many details of the crown, such

as branches and existing variations. However, the lower the spatial resolution, the lower the ability to differentiate the crown area and the soil, especially for trees with reduced crown diameters. Moreover, in these images, the brightness variation in the crown of trees with larger crowns causes greater commission errors (Ke and 2011). Such evidence is in agreement with the results reported by Lausch et al. (2013). In their study, the use of data with higher spatial resolution such as UAV derivatives may provide greater accuracy in classification. The authors researched the effects of spatial resolution on accuracy in the classification of damage caused by bark beetles with larger ground sample distance (GSD, of 4 cm and 7 cm). The smaller GSD (4 cm) provided better classification accuracy since the better results with higher spatial resolutions are probably due to the lower level of mixing of the spectrum of adjacent objects.

Data from the tested classifications indicate that this individual tree-based approach can be trained in larger areas, based on the results of a smaller and representative area, as recommended by Nasi et al. (2015). These authors also recommend using phenological variations of the trees evaluated by time series and checking the calibration and due processing of remotely located data. This concept is therefore, encouraged for further studies allowing a better assessment of the damage over time. Multi-temporal monitoring of a forest stand is recommended since it may indicate new attacks and spatial patterns (Senf et al., 2017). Other spectral ranges, such as near-infrared (NIR) and shortwave infrared (SWIR) (Foster et al. 2016; Abdullah et al. 2018), in medium-resolution spatial or thermal sensors (Junttila et al. 2016) with sensors embedded in UAVs can provide additional information about the health status.

As already described, the classification error between the attacked, non-attacked, and dead trees can be explained by using heterogeneous pixels as a function of spatial resolution, due to the difficulty in separating the crowns and the occurrence of trees with low initial attacked level. This also occurred in the research conducted by Negron-Juarez et al. (2011), which reported the underestimation of tree mortality detection at the subpixel level (small forest gaps) in the Amazon using Landsat-5 data, with a pixel of 30 meters. At higher levels of tree mortality, the accuracy of the single datum classification was higher.

As previously commented by Liebsch et al. (2015) and Liebsch et al. (2018), advancements in managing *Pinus taeda* stands under *Sapajus nigritus* attacks bring new perspectives for both management and conservation initiatives. However, many other factors still need to be considered in the context of forest management initiatives such as food supplementation and surveillance (Mikich and Liebsch, 2014ab).

A better assessment of the tree resources in nearby forest remnants is also strongly recommended as reported by Tujague and Janson (2017). In their research, they argue that forest remnants in the tropics may have very low densities and vary across time in their seasons of peak fruiting and maturation rates. As recommended by Liebsch and Mikich (2017) other tree species that suffer little, or no damage could be serve as buffer zone in forest stands nearby remnants. According to these authors, it also opens new perspectives for the improvement and genetic engineering of *Pinus taeda* stands. However, these authors also pointed out that these strategies shll be combined with the enrichment of native forests in the nearby forest remnants that is generally low.

This research also shows the applicability of high spatial resolution images acquired from UAVs to explore the attack by *Sapajus nigritus*. Further steps could evaluate the applicability of automatic counting methods. It also brings new perspectives for combining photogrammetric techniques and checking the applicability of digital image processing and deep learning (DL) techniques to extract crown attributes from the images. Hence, it allows further analysis of the robustness of the reported approach to count objects and compare it with forthcoming up-to-date methods. Therefore, both the marking point, annotated in the center of each structure and a bounding box annotation using bounding boxes as suggested by Biffi et al. (2021) in commercial apple fruit orchards is recommended here for completeness of comparisons allowing time-demanding performance assessments. Interestingly, it would be to evaluate hyperspectral sensors or cameras acquiring images in additional wavelengths such as NIR, SWIR and thermal, to evaluate better the initial attack stage that still remains a challenge.

CONCLUSION

The best algorithm for classifying the health of *Pinus taeda* L. trees. attacked by *Sapajus nigritus* was the SVM, and the highest accuracy was represented by the composition of the ExG index associated with the original spectral bands. In addition, the results were promising, and replicable and could help in the management of *Pinus taeda* stands attacked by *Sapajus nigritus*. However, more studies and public initiatives are encouraged to revise the quality of the forest remnants nearby these forest plantations.

AUTHORSHIP CONTRIBUTION

Project Idea: CTP, MBS, VPF

Database: VPF, MMP

Processing: CTP

Analysis: CTP, MBS, VL, FDAM

Writing: CTP, VL, FDAM

Review: CTP, MBS

ACKNOWLEDGEMENTS

To FUMDES (Support Fund for the Maintenance and Development of Higher Education) of Santa Catarina for granting the scholarship and the financial assistance. CPNq and FAPESC for the individual grants. CAPES for the support to our graduate program.

REFERENCES

ABDULLAH H.; DARVISHZADEH R.; SKIDMORE A. K.; GROEN T. A., HEURICH M. European spruce bark beetle (*Ips typographus* L.) green attack affects foliar reflectance and biochemical properties. International Journal of Applied Earth Observation and Geoinformation , v. 64, p. 199-209, 2018.

ALVARES, C. A.; STAPE, J. L.; SENTELHAS, P. C.; GONÇALVES, J. L. M.; SPAROVEK, G. Köppen's climate classification map for Brazil. Meteorologische Zeitschrift , v. 22, n. 6, p. 711-728, 2013.

BEHMANN, J.; STEINRÜCKEN, J.; PLÜMER, L. Detection of early plant stress responses in hyperspectral images. ISPRS Journal of Photogrammetric and Remote Sensing , v. 93, p. 98-111, 2014.

DASH, J. P.; PEARSE, G. D.; WATT, M. S. UAV Multispectral Imagery Can Complement Satellite Data for Monitoring Forest Health. Remote Sensing, v. 10, n. 1216, p.1-22, 2018.

DI BITETTI, M. S. Primates bark-stripping trees in forest plantations – A review. Forest Ecology and Management, v. 449, n. 117482, 2019.

ESRI – ENVIRONMENTAL SYSTEMS RESEARCH INSTITUTE. *ArcGIS Professional GIS for the desktop, version 10.7.1*. Available from: https://support.esri.com/en/Products/Desktop/arcgis-desktop/arcmap/10-7-1. Accessed: May 20, 2021.

FOSTER, A. C.; WALTER, J. A.; SHUGART, H. H.; SIBOLD, J.; NEGRON J. Spectral evidence of early-stage spruce beetle infestation in Engelmann spruce. Forest Ecology and Management, v. 384, p. 347-357, 2017.

HANSEN, E. M.; NEGRON, J. F.; MUNSON, A. S.; ANHOLD, J. A. A retrospective assessment of partial cutting to reduce spruce beetle-caused mortality in the southern Rocky Mountains. Western Journal of Applied Forestry, v. 25, n. 2, p. 81-87, 2010.

HUNT, E. R.; DAUGHTRY, C. S. T.; EITEL, J. U. H.; LONG, D. S. Remote sensing leaf chlorophyll content using a visible band index. Agronomy Journal, v. 103, n. 4, p. 1090-1099, 2011.

IBÁ - INDÚSTRIA BRASILEIRA DE ÁRVORES. *Relatório Anual 2021*. Available from: https://iba.org/datafiles/publicacoes/relatorios/relatorioiba2021-compactado.pdf?utm_source=akna&utm_medium=email&utm_campaign=Iba-lanca-Relatorio-Anual-2021. Accessed: Dec 10, 2021.

ISHIDA, T. *et al.* A novel approach for vegetation classification using UAV-based hyperspectral imaging. Computers and Electronics in Agriculture , v. 144, p. 80-85, 2018.

JENSEN, J. R. Remote Sensing of the Environment: An Earth Resource Perspective. 2 ed. Pearson Prentice Hall, Upper Saddle River. 2007.

JUNTTILA, S. *et al.* Effect of forest structure and health on the relative surface temperature captured by airborne thermal imagery–case study in Norway spruce-dominated stands in Southern Finland. Scandinavian Journal Forest Research , v. 32, n. 2, p.154-165, 2016.

KE, Y.; QUACKENBUSH, L. J. A review of methods for automatic individual tree-crown detection and delineation from passive remote sensing. International Journal of Remote Sensing , v. 32, n. 17, p. 4725-4747, 2011.

KOEHLER, A.; FIRKOWSKI, C. Descascamento de pinus por macaco-prego *(Cebus apella*). Floresta , v. 24, n.1-2, p. 61-75, 1996.

LAUSCH, A.; PAUSE, M.; DOKTOR, D.; PREIDL, S.; SCHULZ, K. Monitoring and assessingof landscape heterogeniety at different scales. Environmental Monitoring and Assessment , v. 185, n. 11, p. 9419-9434, 2013.

LIEBSCH, D.; MARQUES, M. C. M.; GOLDENBEG, R. How long does the Atlantic Rain Forest take to recover after a disturbance? Changes in species composition and ecological features during secondary succession. Biological Conservation , v. 141, n. 6, p. 1717-1725, 2008.

LIEBSCH, D.; MIKICH, S. B.; OLIVEIRA, E. B. de.; MOREIRA, J. M. M. Á. P. Descascamento de *Pinus taeda* por macacos-prego (*Sapajus nigritus*): tipos e intensidades de danos e seus impactos sobre o crescimento das árvores. Scientia Forestalis , v. 43, n. 105, p. 37-49, 2015.

LIEBSCH, D.; MIKICH, S. B. Damage caused by brown-capuchin monkeys to nine pinus species and the implications for forest management. Floresta, v. 47, n. 1, p. 37-42, 2017.

LIEBSCH, D.; MOREIRA, J. M. M. Á.; OLIVEIRA, E. B. de.; MIKICH, S. B. Impacto do descascamento de árvores de *Pinus taeda* L. por macacos-prego na produção e receita em plantios com desbastes. BIOFIX Scientific Journal , v. 3, n. 1, p. 48-55, 2018.

LOUHAICHI, M.; BORMAN, M. M., JOHNSON, D. E. Spatially located platform and aerial photography for documentation of grazing impacts on wheat. Geocarto International, v. 16, n. 1, p. 65–70, 2001.

MANCINI, F. *et al.* Unmanned Aerial Vehicles (UAV) for High Resolution Reconstruction of Topography: The Structure from Motion Approach on Coastal Environments. Remote Sensing, v. 5, n. 12, p. 6880-6898, 2013.

MIKICH, S. B.; LIEBSCH, D. O Macaco-prego e os Plantios de Pinus spp. Comunicado Técnico, Embrapa Florestas. Colombo, PR, 234:1-5, 2009.

MIKICH, S. B.; LIEBSCH, D. Assessment of food supplementation and surveillance as techniques to reduce damage caused by black capuchin monkeys *Sapajus nigritus* to forest plantations. Current Zoology, v. 60, n. 5, p. 581-590, 2014a.

MIKICH, S. B.; LIEBSCH, D. Damage to forest plantations by tufted capuchins (*Sapajus nigritus*): too many monkeys or not enough fruits? Forest Ecology and Management , v. 314, p. 9-16, 2014b.

MORIYA, E. A. S. *et al.* Detection and mapping of trees infected with citrus gummosis using UAV hyperspectral data. Computers and Electronics in Agriculture, v. 188, p. 106298, 2021.

NASI, R. *et al.* Using UAV-Based Photogrammetry and Hyperspectral Imaging for Mapping Bark Beetle Damage at Tree-Level. Remote Sensing, v. 7, n. 11, p. 15467-15493, 2015.

NEGRON-JUAREZ, R. I. *et al.* Detection of subpixel treefall gaps with Landsat imagery in Central Amazon forests. Remote Sensing of Environment, v. 115, n. 12, p. 3322-3328, 2011.

NEVALAINEN, O. *et al.* Individual tree detection and classification with UAV-Based Photogrammetric point clouds and hyperspectral imaging. Remote Sensing, v. 9, n. 3, p. 185, 2017.

REDWEIK, P. Fotogrametria Aérea. Universidade de Lisboa (Apostila) 2007.

RETSLAFF, F. M. S.; FIGUEIREDO FILHO, A.; RETSLAFF, F. A. S.; MOLINARI, J. R. A. Crescimento e produção em povoamentos de *Pinus taeda* L. danificados por macacos-prego. Scientia Forestalis , v. 48, n.125, n. e3237, 2020.

ROCHA, V. J. 2000. Macaco-Prego, como controlar essa nova praga florestal? Floresta, v. 30, n. 1-2, p. 95-99, 2007.

SAFONOVA, A. *et al.* Detection of Fir Trees (*Abies sibirica*) Damaged by the Bark Beetle in Unmanned Aerial Vehicle Images with Deep Learning. Remote Sensing , v. 11, n. 6, p.1-19, 2020.

SENF, C.; SEIDL, R.; HOSTERT, P. Remote sensing of forest insect disturbances: Current state and future directions. International Journal of Applied Earth Observation and Geoinformation, v. 60, p. 49-60, 2017.

SYLVAIN, J. D.; DROLET, G.; BROWN, N. Mapping dead forest cover using a deep convolutional neural network and digital aerial photography. ISPRS Journal of Photogrammetry and Remote Sensing, v. 156, p. 14-26, 2019.

TUJAGUE, M. P.; JANSON, C. H. Wild capuchin monkeys anticipate the amount of ripe fruit in natural trees. Animal Cognition, v. 20, p. 841-853, 2017.

VOGELMANN, J. E.; TOLK, B.; ZHU, Z. L. Monitoring forest changes in the southwestern United States using multitemporal Landsat data. Remote Sensing of Environment, v. 113, n. 8, p. 1739–1748, 2009.

ZARCO-TEJADA, P. *et al.* Assessing vineyard condition with hyperspectral indices: Leaf and canopy reflectance simulation in a row-structured discontinuous canopy. Remote Sensing of Environment, v. 99, n. 3, p. 271–287, 2005.

WOEBBECKE, D. M.; MEYER, G. E.; VON BARGEN, K.; MORTENSEN, D. A. Color indices for weed identification under various soil, residue, and lighting conditions. Transactions of the ASAE, v. 38, n. 1, p. 259–269, 1995.